Maneuver Detection Using the Radar Range Rate Measurement

David F. Bizup, Donald E. Brown

November 25, 2002

Abstract

Tracking maneuvering targets with radar is complicated because radar cannot measure target accelerations. We use the range rate measurement to calculate a new statistic that is a surrogate measurement of target acceleration under a coordinate turn model. Its distribution is found via simulation. A threshold test of the statistic turns out to be a reliable detector of a maneuver, and its receiver operating characteristic is found. A tracker that uses a threshold test of the new statistic of accelerations to detect maneuvers and set the state noise in a Kalman filter tracker is devleoped and compared to other, common maneuvering track filters. The new method outperforms a two mode interacting multiple model tracker and a noise switching tracker that switches based on the position measurement residuals.

Keywords: Kalman filter, radar tracking, maneuver tracking, radial velocity, range

1 INTRODUCTION

Radar target tracking involves measurement, association and filtering. Radar measures a target's range, one or two angles, and its range rate. Range rate, also called the Doppler or radial velocity, is the velocity along a line extending from the radar to the target. Tracks are data structures containing estimates of relevant target characteristics, including its position and velocity. Association algorithms link radar measurements to existing tracks by comparing the measurements to the track state estimate. The associated measurements are filtered to update the track state estimates over time. The Kalman filter and its derivatives like the $\alpha\beta$ filter are common track filters.

Although the range rate measurement is used to associate measurements to tracks [1], it is not usually used to filter the state estimate. The reason is simple: it is highly nonlinear with respect to a Cartesian state space. Extending a Kalman filter tracker to account for the nonlinearities is reported to work well sometimes [1], but fails to provide satisfactory results for all target trajectories [2]. Most trackers simply ignore range rate when filtering the state estimate. Consequently, they are not using all of the information provided by the radar.

Tracking maneuvering targets is an important problem complicated by the fact that the accelerations acting on the target are not measurable with radar [3]. A variety of techniques have been developed to detect manevuers and adjust the track filter to compensate for them. Three common techniques are mode switching, input estimation, and interacting multiple models. Their common feature is that they use the position measurement twice; first to detect or estimate the probability of a maneuver, then again to update the track state estimate. This type of data reuse can induce large errors when the measurement is noisy. When the measurement noise is high, the tracker's gain is increased, the noisy report is weighted more than it should be, and the track jumps far from the actual target position.

Mode switching trackers [2] monitor the sequence of position measurement residuals to determine whether a target is maneuvering. The residuals are subject to statistical tests for detecting trends or instantaneous changes in the target's trajectory. If the tests indicate that a maneuver has occured then the gain or state noise covariance level is increased to improve tracking during the maneuver. Otherwise, the gain is set low to dampen the measurement noise. When incorrect associations are frequent, such as in the presence of multiple targets or chaff, mode switching trackers perform poorly.

Input estimation trackers model maneuvers as exponentially correlated accelerations. The time a maneuver started and the acceleration causing it are estimated from the position measurement residuals. The filter parameters are changed to match the estimated acceleration. These filters require a historical record of the track and measurements to estimate the autocorrelation. In [4], a tracker using data from a sliding window 12 scans long is presented and analyzed. Simulation results show that this tracker follows maneuvers well, but the requirement to store a large number of data and wait 12 scans for optimal tracking may make it impractical for real time trackers.

Interacting Multiple Model (IMM) trackers hypothesize two or more maneuver maneuver modes and assume that the mode changes are modeled by a hidden Markov process. The measurements are filtered through each mode to produce a set of state estimates conditioned on the hypothesized maneuver mode. The

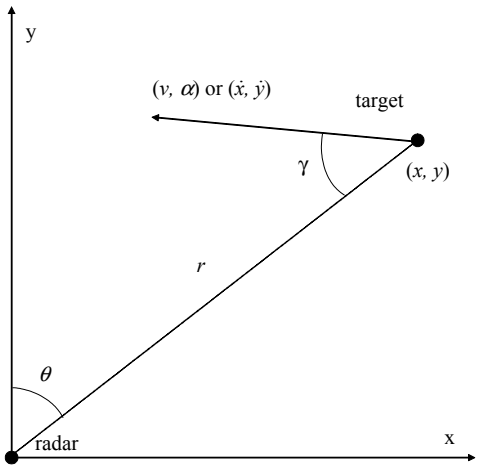

Figure 1: Problem space: Cartesian frame with radar fixed at the origin and a moving target.

outputs are then combined as a weighted sum where the weights are proportional to mode likelihoods [5]. The most basic IMM [6] has one low acceleration mode and one high acceleration mode and assumes that that the Markov chain transition probabilities are stationary and known. More complicated IMMs can have nonstationary transition probabilities, autocorrelated maneuvers, and adaptive mode sets [5]. They perform well when the modes accurately represent the true accelerations and are relatively robust to small modelling errors. Their computational complexity increases linearly with the number of maneuver modes.

This paper develops a new statistic of accelerations based on the range rate measurement, not the position measurement residuals. The statistic turns out to be a reliable indicator of a maneuver and a good estimator of the acceleration. In section II, the statistic is derived from a coordinated turn manevuer model. In section III, its distribution function is evaluated via simulation. In section IV, a mode switching tracker using the new statistic is compared to a mode switching tracker using the position measurement residuals and a two mode IMM. Section V is a summary of significant results.

2 A STATISTIC OF ACCELERATIONS

A. Problem Formulation

The problem is formulated in a two dimensional Cartesian frame where the x and y axes are in the east and north directions, respectively, as in figure 1. The target is allowed to move anywhere in the plane. It maintains a constant velocity in the interval $(0, t_{k-1}]$. At t_{k-1} it begins a coordinated turn that lasts at least until t_k. Position is described by the coordinate pair (x, y). Velocity can be described by either speed and heading (v, α) or the component velocites in the directions of the axes $\left(\dot{x}, \dot{y}\right)$. In a Cartesian system, the

component representation is the most natural and easiest to implement so we describe the target state at time t_k by the vector $s_k = \left[\begin{array}{cccc} x & y & \dot{x} & \dot{y} \end{array} \right]_k^T$. The statistic of accelerations is calculated using the speed and heading. The relation between these representations is

$$v = \sqrt{\dot{x}^2 + \dot{y}^2} \tag{1}$$

$$\alpha = \arctan\left(\frac{\dot{x}}{\dot{y}}\right) \tag{2}$$

The radar is stationary, fixed at the origin, and rotates at a constant angular velocity. It measures the target's bearing θ, range r,and range rate $\dot{r}$. Range and bearing are converted to x and y in the usual manner. The pseudo measurement

$$z_k = \left[\begin{array}{c} x_m \\ y_m \\ \dot{r}_m \end{array} \right]_k = \left[\begin{array}{c} x \\ y \\ \dot{r} \end{array} \right]_k + u_k \tag{3}$$

is the input to the association and filtering algorithms, where subscript k denotes the k^{th} measurement which is taken at time t_k, subscript m denotes a measured value, and u_k is the measurement error. Measurement errors are assumed to be white Gaussian noises with known variances $\sigma^2_{r,k}$, $\sigma^2_{\theta,k}$ and $\sigma^2_{\dot{r},k}$.

Range rate is the component of target velocity in the direction of a line extending from the radar to the target. In figure 1, γ denotes the difference between the inverse bearing and target heading,

$$\gamma_k = \alpha_k - (\theta_k + \pi_k) \tag{4}$$

It is clear that the range rate equals the negative product of speed and cosine of γ_k

$$\dot{r}_k = -v_k \cos(\gamma_k) \tag{5}$$

In terms of the track state vector

$$\dot{r_k} = \frac{x_k \dot{x}_k + y_k \dot{y}_k}{\sqrt{x_k^2 + y_k^2}} \tag{6}$$

Given the target state the range rate is uniquely determined. However, it is clear from (6) that given the range rate the target state can have infinitely many values. In the next two parts of this section, we propose a maneuver model, place some reasonable restrictions on acceleration, and find a finite number of solutions to (6). The solutions represent accelerations that could have acted on the target.

B. Maneuver Model

The target is assumed to start at time 0 and move with a fixed speed and heading until t_{k-1}, the time of the $(k-1)^{th}$ measurement. At t_{k-1} it either continues at the same speed and heading or makes a coordinated turn that lasts at least until t_k. Thus, in the interval $(t_{k-1}, t_k]$ the target is acted upon by either no acceleration or a constant centripetal acceleration.

A constant centripetal acceleration acting on a moving body induces constant speed circular motion. If the target turns, its speed is constant and its trajectory is a circular arc whose radius of curvature depends on both target speed and the strength of the acceleration. The arc's length equals the distance the target traveled, $v_{k-1}(t_k - t_{k-1})$, and its angular width equals the ratio of its length to its radius of curvature. Speed is constant, so the arc is swept at a constant angular rate. Target heading is always tangential to the path. Therefore, heading also changes at a constant angular rate and the total change in heading equals the angular arc width.

C. Calculating the Statistic of Accelerations

Given the target's initial position and component velocities, and the strength and duration of the acceleraion, the target's final state is uniquely determined. When the state is known the range rate, relative to a radar at the origin, is uniquely determined by (6). However, infinitely many states have the same range rate. Even if the initial state s_{k-1} and turn duration $(t_k - t_{k-1})$ are known with certainty, there are many accelerations that result in the same range rate. Therefore the mapping from acceleration to range rate $\dot{r}_k$ is many-to-one. In fact, if the accelerations are allowed to be arbirtarily large, the mapping is infinitely-many-to-one. Conversely, it is true that conditional on initial state s_{k-1}, the model provides a one-to-many mapping from the final range rate r_k to the accelerations that might have been acting on the target. We limit the number of possible accelerations by requiring that the target's change in heading is no more than 360° between radar measurements.

Two methods for calculating the statistic of accelerations are provided; one exact, the other using an approximate bearing. The exact method requires the solution of a nonlinear optimization problem. In the approximate method, the bearing to the target is assumed equal to the projected bearing at t_k for every acceleration. This assumption simplifies the problem considerably without inducing too much error. The approximate method is described first, then the exact method, then the errors are shown to be small by example.

D. Approximate Method

The statistic of accelerations was first introduced in [7]. It is calculated by conditioning on the previous state estimate s_{k-1} and finding the accelerations that would have resulted in states with range rates equal to the measured range rate. First, range rate is mapped to a set of target headings. These are mapped to a set of possible heading changes. Heading change equals the target trajectory's angular arc width, so each heading change corresponds to exactly one arc. The radii of curvature of these arcs can be determined. Finally, the radii are mapped to accelerations.

Given the previous state estimate s_{k-1}, the current range rate measurement $\dot{r}_{m,k}$, and assuming that the maneuvers are coordinated turns, the statistic $\underset{\sim}{\mathbf{c}}$ is calculated as follows. The target's speed is known

$$v_k = v_{k-1} = \sqrt{\dot{x}_{k-1}^2 + \dot{y}_{k-1}^2} \tag{7}$$

The angular difference between the inverse bearing and heading is determined by solving (5) for γ

$$\gamma_k = \arccos\left(-\frac{\dot{r}_k}{v_k}\right) \tag{8}$$

The cosine function is symmetric so if the bearing θ_k is known then there are two possible headings that solve (4), $\alpha_k = (\theta_k + 180°) \pm \gamma_k$.

If the target is far from the radar, its speed is not too large, and the radar scan rate is sufficiently fast then the bearing does not change much and it can be approximated by

$$\theta_k \approx \arctan\left(\hat{x}_k / \hat{y}_k\right) \tag{9}$$

where $\left(\hat{x}_k, \hat{y}_k\right)$ is the position estimate projected forward in time to the latest measurement. The measured position error is dominated by the bearing error, so equation (9) is probably a better estimate of the true

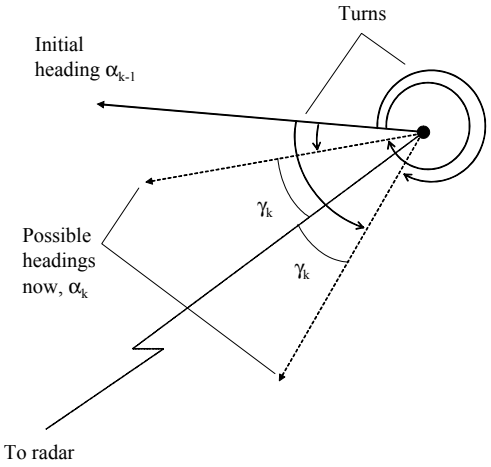

Figure 2: Four possible turns, two to the left and two to the right, such that the actual and measured range rates are equal.

bearing than the latest measurement. Examples that shows the reasonableness of this approximations are provided after the statistic is fully developed.

Figure 2 shows four turns that take the target from its initial heading α_{k-1} to α_k. Either heading can be attained by a turn to the left or to the right. More maneuvers are possible if the target can make more than one complete revolution between radar measurements. By restricting the analysis to turns of less than one revolution, there are only four possible maneuvers. Denoting the heading changes for these maneuvers by $\underset{\sim}{\tau}$, so that $\tau_{left} = \left(\alpha_{k-1} - \underset{\sim}{\alpha}_k\right) \bmod (360)$ and $\tau_{right} = \left(\underset{\sim}{\alpha}_k - \alpha_{k-1}\right) \bmod (360)$, and sorting appropriately, yields a four-vector of possible turns

$$\underset{\sim}{\tau}_k = \begin{bmatrix} \tau_{\text{max left}} \\ \tau_{\text{min left}} \\ \tau_{\text{min right}} \\ \tau_{\text{max right}} \end{bmatrix}_k^T \tag{10}$$

Recall that the trajectories are circular arcs whose angular widths equal heading change. Therefore, $\underset{\sim}{\tau}_k$ can be interpreted as one-to-four mapping from range rate to heading change, where the heading changes are restricted to be less than 2π. Radius of curvature equals the ratio equal the ratio of the angular arc width to arc length. Denoting the radii $\underset{\sim}{\rho}$,

$$\underset{\sim}{\rho}_k = \frac{v_k \left(t_k - t_{k-1}\right)}{\underset{\sim}{\tau}_k} \tag{11}$$

where the division is understood to be on an element by element basis. It is well known that centripetal acceleration is the ratio of speed squared to the radius of curvature. There are four accelerations that cause

turns resulting in the measured range rate,

$$\underset{\sim}{\mathbf{c}}_k = \frac{v_k^2}{\underset{\sim}{\boldsymbol{\rho}}_k} \tag{12}$$

The elememts of $\underset{\sim}{\mathbf{c}}_k$ are the magnitudes of the accelerations that could have acted upon the target

$$\underset{\sim}{\mathbf{c}}_k = \begin{bmatrix} c_{\text{max left}} \\ c_{\text{min left}} \\ c_{\text{min right}} \\ c_{\text{max right}} \end{bmatrix}_k^T \tag{13}$$

$\mathbf{c}_k$ is then scaled to g's, where $1g = 9.8m/s^2$. As shown in sections III and IV, the minimum of these values

$$c_{\min,k} = \min\left(\underset{\sim}{\mathbf{c}}_k\right) \tag{14}$$

is a statistic that turns out to be a reliable indicator of a maneuver, and a good predictor of the strength of the maneuver over a wide range of accelerations.

E. Exact Method

If the target accelerates in the interval $(t_{k-1}, t_k]$ then equation (9) is not exact. Additionally, the set of resultant bearings, conditional on each of the four possible accelerations, are not equal as assumed in the computataion of possible turn angles. Therefore, the elements of $\underset{\sim}{\mathbf{c}}_k$ are not the exact accelerations that may have acted on the target to produce to measured range rate.

The exact bearings and accelerations, conditional on the initial state and the current range rate, can be determined but the algorithm is considerably more complicated and requires the solution of four nonlinear optimization problems. The algorithm for calculating the exact accelerations follows.

Consider a target with initial position (x, y), speed v, heading α, and constant acceleration a. Recall that its trajectory is a circular arc with radius $\rho(a)$ and angular width $\tau(a)$ where $\rho(a)$ and $\tau(a)$ are given by equations (12) and (11), respectively. Let $(x_0(a), y_0(a))$ denote the focal point of the arc, or the center of the circle containing the trajectory. It lies on a line that passes through (x, y) and is perpendicular to α. The target's final state is found by rotating it about the focal point by $\tau(a)$. Denoting the system of linear equations for the rotation by $R(a)$, the final state is

$$s_k(a) = R(a) \begin{bmatrix} x - x_0(a) \\ y - y_0(a) \\ \dot{x} \\ \dot{y} \end{bmatrix} + \begin{bmatrix} x_0(a) \\ y_0(a) \\ 0 \\ 0 \end{bmatrix} \tag{15}$$

The range rate, $\dot{r}(a)$, is uniquely determined by equation (6). The magnitude of the largest allowable acceleration, denoted a^* corresponds to a change in heading of 360° and can be found by equations (11) and (12). The elements of $\underset{\sim}{\mathbf{c}}_k$ are the four solutions to the optimization problem

$$\min_{0 \le a \le a^*} \quad \dot{r}(a) - \dot{r}_m \tag{16}$$

where two solutions correspond to left turns and two to right turns. $c_{\min}$ is the minimum of $\underset{\sim}{\mathbf{c}}_k$.

F. Comparison of Exact and Approximate Methods

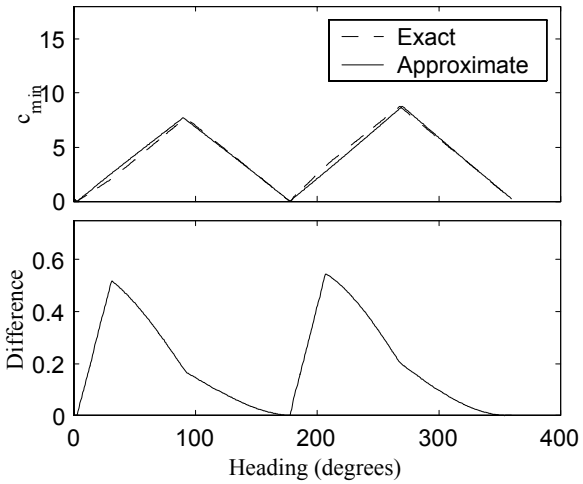

Figure 3: $c_{\min}$ computed using the exact and approximate method (top), and their absolute differences (bottom) for a 1000 kn target at 50 nmi.

The differences in $c_{\min}$ calculated by the approximate and exact methods arise because of the assumption in equation (9). The approximation error in (9) is bounded above by the largest possible change in bearing given the target state and the radar scan rate. It increases with increasing speed and scan period, or with decreasing range. Two examples show the differences between the approximate and exact methods. The first example is intended to induce large differences. The target is close and fast, and the radar scans slowly. The second example is intended to induce smaller differences. The speed, range, and radar scan rate are moderate.

In the first example, the target is at $1000kn$ and $50nmi$, and the radar has a scan period of $10s$. The state estimate s_{k-1} always has the target due north of the radar, the measured range rate $\dot{r}_{m,k}$ always equals $100kn$ and heading is varied from 0 to 360°. $c_{\min}$ values, calculated using the exact and approximate methods, and their differneces are shown in figure 3. The top graph shows $c_{\min}$ as a function of target heading for the exact and approximate methods. The bottom graph shows their absolute differences. In the second example, the target is at $400kn$ and $150nmi$, and the radar has a scan period of $4s$. The target is always due north of the radar, $\dot{r}_{m,k}$ always equals 100 kn, and heading is varied form 0 to 360°. The results are shown in figure 4. The differences in the second case are pracitally and visually negligible. They are a full order of magnitude lower than those in the first case.

G. Remarks

Consider the four maneuvers shown in figure 2. The acceleration of the smallest turn to the left is much less than that of the others. No matter which turn the target actually makes, $c_{\min}$ will approximately equal the acceleration causing the smallest turn. If the target maneuvers are not too strong, $c_{\min}$ is expected to be a good estimate of the actual acceleration and its distribution should have a mode near the actual acceleration. If the maneuvers are large then $c_{\min}$ is expected to underestimate the acceleration. Its distbritution may have a mode near the actual acceleration and it could have multiple modes at lower accelerations. This behavior is demonstrated via simulation in section III.

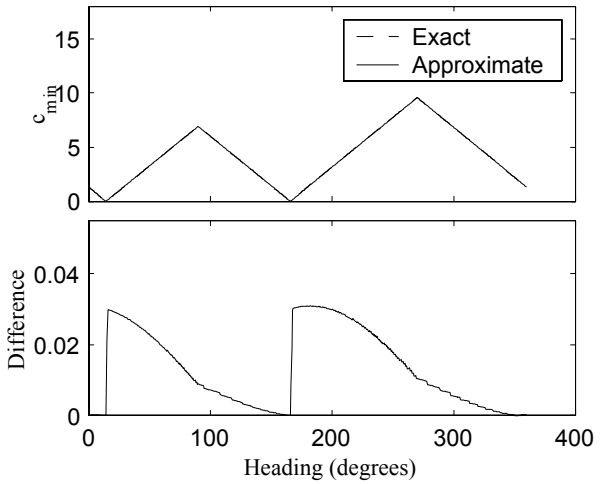

Figure 4: $c_{\min}$ computed using the exact and approximate method (top), and their absolute differences (bottom) for a 400 kn target at 150 nmi.

The maneuver model assumes that target speed is constant between measurements. If the speed increases or the range rate measurement is very noisy then the measured range rate might exceed the estimated velocity. In that case (8) has no solution. Any filter that uses $c_{\min}$ should check for this condition.

If the range rate measurement errors are independent of the range and bearing measurement errors as assumed, then $c_{\min}$ is independent of the radar position measurements. Because of this independence, a track filter that uses $c_{\min}$ for maneuver detection and estimation might have considerable advantage over maneuvering target trackers that use the sequence of position measurement residuals. In those trackers, very noisy position measurements, or outliers, cause false alarms. The probability that the measurement is an outlier given a false alarm is high. In a tracker using $c_{\min}$, false alarms are caused by range rate measurement outliers. The probability of a position measurement outlier given a false alarm is low because the position and range rate measurements are independent.

There is evidence that range and range rate measurement errors are correlated [8]. In this case, a tracker using $c_{\min}$ still has an advantage. First, the joint probability of range rate and position measurent outliers is still less than the probability of a position measurement outlier alone. Secondly, the range errors are usually small relative to bearing errors. A false alarm does not degrade the state estimate much unless the bearing error is also an outlier.

3 THE DISTRIBUTION OF $c_{\min}$

A. Tracking Simulation

The mapping from range rate to $c_{\min}$ defined by (7) to (14) is both one-to-many and nonlinear with respect to the state space. The distributional form of the range rate measurement error is not preserved, and may be impossible to calculate analytically. The distribution of $c_{\min}$ is evaluated via simulation.

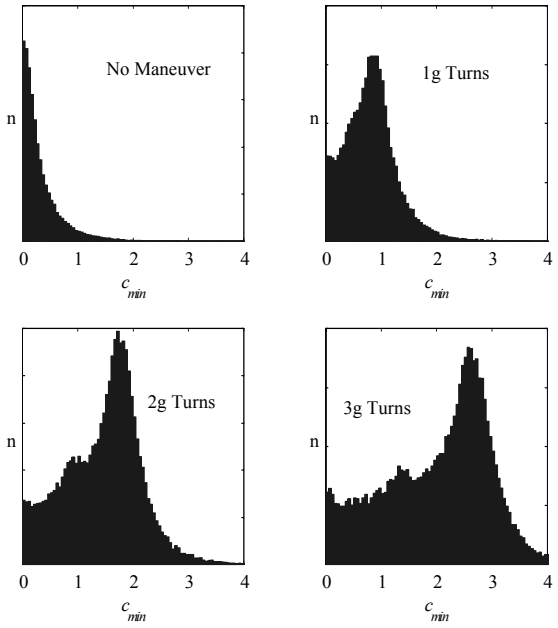

Figure 5: Histograms of $c_{\min}$ for 0 to 3g turns with varying target range, speed, heading, and turn direction. 84,000 samples per histogram.

The distribution of $c_{\min}$ depends on target speed, heading relative to the bearing line, range at the time the maneuver starts, the strength and direction of the turn, the distribution of range rate measurement errors and the radar scan rate. It does not depend on the bearing to the target at the start of the maneuver because the tracking problem is invariant under rotation. A target tracking simulation that varies these parameters was used to find the empirical distribution of $c_{\min}$.

The empirical density functions reported in this section are for a simulated radar that is fixed at the origin, has a scan period of 10s, and has white, Gaussian measurement errors with standard deviations $\sigma_r = 100$ ft, $\sigma_\theta = 3°$ and $\sigma_{\dot{r}} = 2\ kn$. The target's speed varies from 200 to 800 kn in 100kn increments, relative heading from 0 to 330° in 30° increments, and range at the start of the maneuver from 50 to 250nmi in 50nmi increments. The target turns either right or left with accelerations from 0 to 7g in 1g increments. A 0g acceleration is equivalent to no maneuver.

The target is tracked using a single mode, uniform motion Kalman filter tracker. The state noises are modeled as white, Gaussian accelerations in the x and y directions with covariances equal to 0.03g. The target travels for 300s at a constant speed and heading then starts its turn. For a radar with a 10s period, the target is detected 30 times before the maneuver starts. This is adequate to let the initial, transient track errors stabilize. The 31^{st} detection is the first detection after the maneuver starts.

B. Empirical Distributions

The simulation was run 100 times for each combination of factors and the sequences of $c_{\min}$ for each run were collected. The histograms shown in figures 5 and 6 were constructed on the values of $c_{\min}$ taken

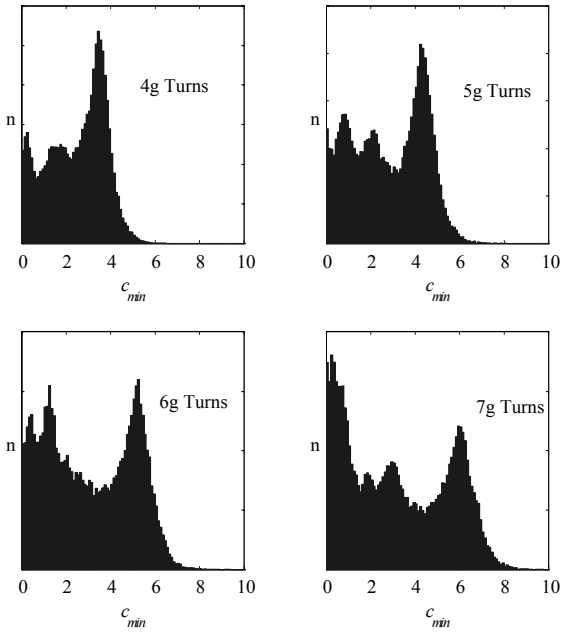

Figure 6: Histograms of $c_{\min}$ for 4 to 7g turns with varying target range, speed, heading, and turn direction. 84,000 samples per histogram.

at the first detection after the maneuver started. They are empirical probability densities of $c_{\min}$ conditional on the acceleration, but unconditional on the other parameters. They exhibit the expected characteristics described at the end of section 2. The distributional form of the range rate errors is not preserved. For small accelerations, the densities have a pronounced mode at the actual acceleration. For larger accelerations, the densities have pronounced modes at the actual acceleration and at some smaller accelerations. At 2g, three modes are apparent. At 4g, the lower modes are quite pronounced. At 6g, the lower modes nearly equal the mode at the actual acceleration. For all accelerations 1g and above, it is apparent that $c_{\min}$ tends to underestimate the acceleration and has expected value less than the actual acceleration, as described at the end of section II.

C. Receiver Operating Characteristic

Suppose that a simple, threshold test of $c_{\min}$ is used to detect maneuvers. If $c_{\min}$ exceeds the threshold then a maneuver is declared. Otherwise, the target is considered nonmaneuvering. In this case, the test of $c_{\min}$ is a deterministic predictor of a binary event. It is a signal detector and can be analyzed as such. In particular, its receiver operating characteristic (ROC) can be determined.

The ROC for a threshold test of $c_{\min}$ using the simulation data for all maneuvers from 0 to 4g is shown in figure 7. Probability of detection is the probability that the threshold is exceeded conditional on the target maneuvering. Probability of false alarm is the probability that the threshold is exceeded conditional on the target not maneuvering. The curve is determined by varying the threshold then counting the number of detections and false alarms at each threshold.

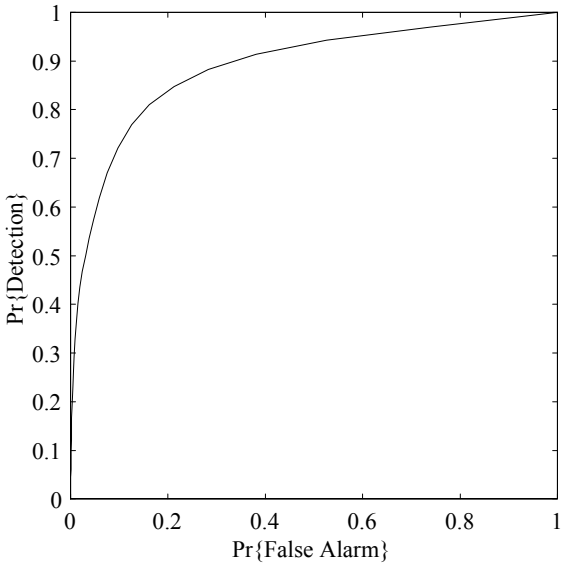

Figure 7: ROC for a threshold test of $c_{\min}$.

Once the ROC is known, it can be used to set the detection threshold in a Bayesian decision system. The system consists of the actual target maneuver state and the test statistic. The relative losses for each combination of target state and test statistic must be determined. The target has two states: maneuvering and nonmaneuvering. The test statistic also has two states: it indicates maneuver or no maneuver. When the target is nonmaneuvering, then the system is said to be in the quiet state if the test statistic indicates no maneuver and in the false alarm state otherwise. If the target is maneuvering, then the system is said to be in the missed event state if the test statistic indicates no maneuver and in the event detected state otherwise. We denote the losses associated with these states $\mathcal{L}_Q$, $\mathcal{L}_{FA}$, $\mathcal{L}_{ME}$, and $\mathcal{L}_D$, respectively. For any threshold, the expected loss is the sum of the losses of each event multiplied by the probability of the event. All the probabilities can be determind from the ROC curve. The Bayes optimal threshold is the value that minimizes the expected loss.

Suppose that the losses are judged to be $\mathcal{L}_Q = 0$, $\mathcal{L}_{FA} = 1.1$, $\mathcal{L}_{ME} = 1.33$, and $\mathcal{L}_D = 1$. It might help to think of losses as relative degradations in track quality. For example, we can interpret these losses to mean that the track is degraded somewhat when the maneuver is detected, by about one tenth more if there is a false alarm, and by one third more if the maneuver is missed. In this case, the optimal threshold is about $1.0g$. If we judge that the degradation during a false alarm is one fifth less than during a detected maneuver so that $\mathcal{L}_Q = 0$, $\mathcal{L}_{FA} = 0.8$, $\mathcal{L}_{ME} = 1.33$, and $\mathcal{L}_D = 1$, then the optimal threshold is about $0.9g$. If the loss of a missed event is judged twice as bad so that $\mathcal{L}_Q = 0$, $\mathcal{L}_{FA} = 1.1$, $\mathcal{L}_{ME} = 2.0$, and $\mathcal{L}_D = 1$, then the optimal threshold is also about $0.9g$.

4 COMPARISON TO OTHER TRACK FILTERS

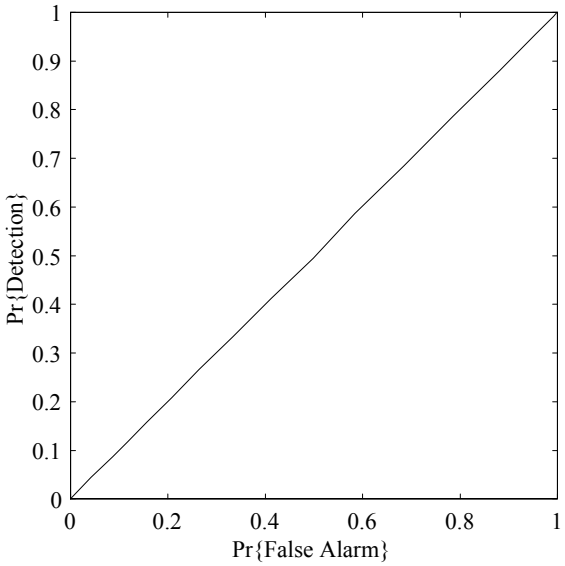

Figure 8: ROC for a threshold test of a fading memory average of position residuals.

A single mode, Kalman filter tracker that switches the state noise covariance based on a threshold test of $c_{\min}$ is tested against two other maneuvering track filters. The first is the single mode, Kalman filter tracker that switches the state noise level based on a threshold test against a fading memory average (FMA) of the position measurement residuals described in [2], [9]. The second is the two mode interacting multiple model (IMM) described in [6]. Both modes are Kalman filter trackers modeling uniform motion with random accelerations. One mode has a low state noise covariance, the other a high covariance. In each tracker, the low and high state noises are $\sigma^2_{low} = 0.0306g$ and $\sigma^2_{high} = 0.6122g$. These values are taken from [6].

The radar model used to evaluate the distribtion of $c_{\min}$ was also used for this comparison. Detection was perfect, so radar measurements are avaiable about once every 10 s. To ensure a fair test, all three trackers started tracks the same way and were run against the same sets of simulated radar data. The tracks were started using a two hit startup rule. For the next 17 detections a uniform motion Kalman filter with low noise covariance updated the track state estimate. The purpose of the 17 detection startup period was to let the initial track errors stabilize. Up until the 19^{th} measurement the track estimates are identical. Starting with the 20^{th} measurement, the trackers can produce different solutions.

In the two single mode trackers, the state noise is set based on a statistical threshold test. If the statistic exceeds the threshold then the $\sigma^2_k = \sigma^2_{high}$, otherwise $\sigma^2_k = \sigma^2_{low}$. The $c_{\min}$ tracker tests $c_{\min}$ against a threshold of $1.0g$. The FMA tracker tests a fading memory average of the position measurement residuals. The residuals, denoted e_k, are the Euclidian distances in nmi between the pseudo-measurements $(x_{m,k}, y_{m,k})$ and the estimate $\left(\hat{x}_k, \hat{y}_k\right)$ given the first $k-1$ measurements. The fade rate is not specified in [2], [9]. We set it to 0.25, so the test statistic is

$$FMA_k = 0.25e_k + 0.75FMA_{k-1} \tag{17}$$

Like the threshold test of $c_{\min}$, the threshold test of the fading memory average of the position

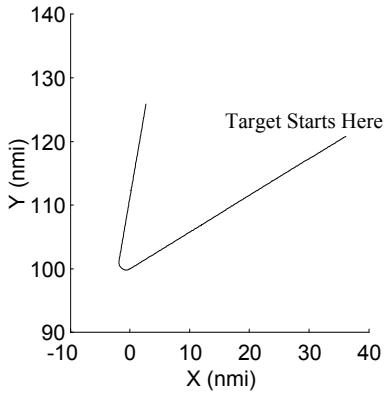

Figure 9: Target trajectory 1: 500 kn target making a 3g turn.

measurement residuals can be interpreted as a signal detector. We computed its ROC via simulation. The results are shown in figure 8. The target parameters were the same as those used to determine the ROC of the of the $c_{\min}$ test, and each combination was run 100 times. The threshold was varied from 2 to $15nmi$. For all practical purposes, the test is noninformative. Choosing a threshold is essentiallly the same as choosing the probability of declaring a maneuver, and then declaring them at random. The Bayes optimal threshold for the noninformative FMA test is easy to determine. Letting p denote the probability of declaring a maneuver, the expected loss is

$$p\left(\mathcal{L}_Q + \mathcal{L}_{ME}\right) + (1-p)\left(\mathcal{L}_{FA} + \mathcal{L}_D\right) \tag{18}$$

If $\mathcal{L}_Q + \mathcal{L}_{ME} > \mathcal{L}_{FA} + \mathcal{L}_D$, then the optimal rule is to never declare a maneuver, which is accomplished by choosing a very large threshold. If $\mathcal{L}_Q + \mathcal{L}_{ME} < \mathcal{L}_{FA} + \mathcal{L}_D$, then always declare a maneuver by choosing a very small threshold. We set the threshold to $8nmi$.

The test performs so poorly because it uses the Euclidean distance of the position residuals instead of a statistical distance. Bearing errors induce larger position errors at longer ranges. Therefore, if there are two targets flying identical trajectories but at different ranges, and the measurement errors against them are the same, the test statistic will be larger for the farther track.

The IMM has a nonmaneuvering mode with state noise covariance σ^2_{low} and a maneuvering mode with covariance σ^2_{high}. The mode transitions are assumed to follow a Markov chain with transition probability matrix

$$P = \begin{bmatrix} .9 & .1 \\ .33 & .67 \end{bmatrix} \tag{19}$$

These transition probabilities, and the noise covariance levels, are taken from [6].

Time series charts of position and speed errors for the three trackers are shown in figures 10, 11, 13, and 14. There are no difference between trackers during the startup period, so the time axes start at $200s$. The charts show the mean error and empirical 95% confidence bounds for 100 simulation runs.

A. Test Case 1: 3g Maneuver

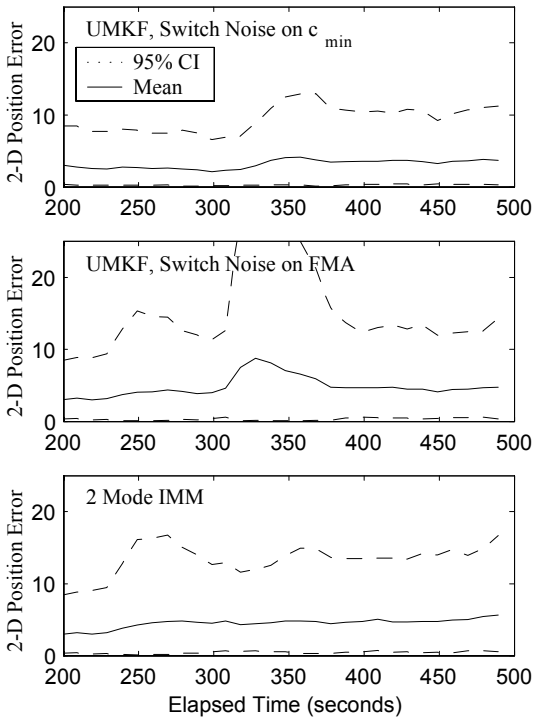

Figure 10: Mean and 95% confidence bounds of position error for the target in test case 1. From top to bottom (i) mode switching tracker using $c_{\min}$; (ii) mode switching tracker using innovation FMA; (iii) 2 mode IMM tracker.

In the first scenario, the target starts at time 0 and travels at $500kn$ on a heading of 240°. After $300s$ the target is $100nmi$ from the radar. It makes a coordinated turn to the right with a $3g$ acceleration for $20s$, and then travels straight for $180s$ as shown in figure 9. The position and speed errors are shown in in figures 10 and 11, respectively.

The tracker switching on $c_{\min}$ outperforms the other trackers on all measures of performance that can be evaluated with these graphs: position error mean and variance, speed error mean and variance, errors during the first straight track segment, during the maneuver, and after the maneuver.

After the warmup period ends, the only difference between the mode switching trackers is the statistical test used to set the state noise covariance. They produce identical solutions until one, but not both, declares a maneuver. From then on, the solutions are different. The tracker switching on $c_{\min}$ consistently outperforms the tracker switching on position measurement residuals. Therefore, the test on $c_{\min}$ is a better indicator of a maneuver in the sense that it has fewer false alarms and more correct detections. In this scenario, the $c_{\min}$ test produces false alarms at a rate of 0.004, the position error test produces them at a rate of 0.55.

When a false alarm occurs the tracker gains are increased and the track state estimate jumps far from the actual target position. The speed estimate increases to account for the large change in the position. At the

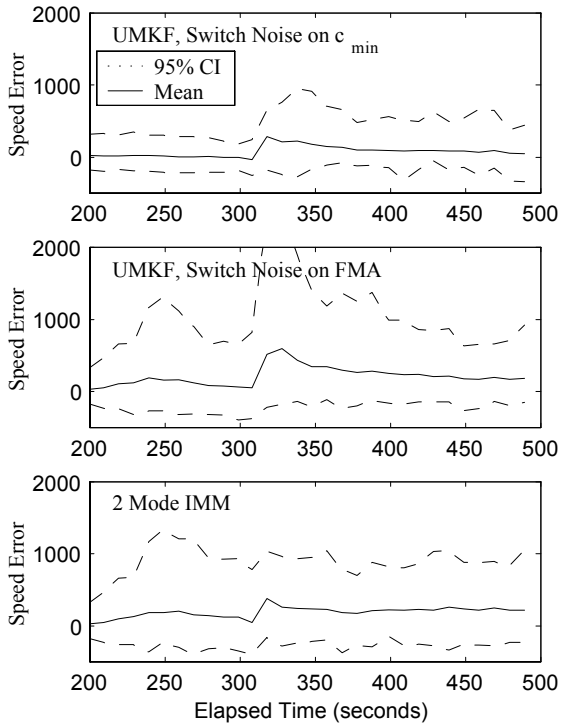

Figure 11: Mean and 95% confidence bounds of position error for the target in test case 1. From top to bottom (i) mode switching tracker using $c_{\min}$; (ii) mode switching tracker using innovation FMA; (iii) 2 mode IMM tracker.

next scan, the position error equals the sum of the position error at the previous scan and the integrated speed error. If the predicited state error or time between measurements is large enough, then the probability of a false alarm increases even if the next measurement is not very noisy. In this way, the effects of a false alarm are propagated through the system, the position errors will be high, and the track speed tends to overestimate the target speed.

During the maneuver, two factors account for the difference between trackers. First, the tracker switching on $c_{\min}$ has a better solution, on average, just before the maneuver starts. It is reasonable to expect it to track better during the maneuver. Secondly, the tracker switching on $c_{\min}$ detects maneuvers more quickly. In all 100 simulation runs, the $c_{\min}$ test detected the maneuver on the first scan after it started. The position residual test detected it on the first scan only 63 times.

The $c_{\min}$ tracker's position and speed error means and variance are consistently lower than the IMM's. The most startling differences are in the speed errors during the first straight track segment. The $c_{\min}$ tracker's mean error is near 0, but the IMM tends to overestimate the speed. The IMM overestimates speed because part of its solution is conditioned on the false hypothesis that the target is maneuvering. The position

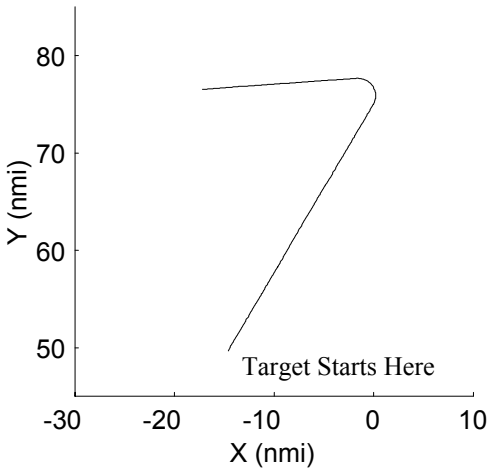

Figure 12: Target trajectory 2: 500 kn target making a 3g turn.

estimate changes by more than the target actually moves, and $\left(\hat{\dot{x}}_k, \hat{\dot{y}}_k\right)$ increase to compensate for the long jumps.

The performance differences between the $c_{\min}$ tracker and the IMM are harder to explain because the trackers compensate for maneuvers differently. Switching trackers are determinstic predictors. They make a decision about whether the target is maneuvering, and then proceed as if that decision is correct. IMMs are probabilistic predictors. Their output is a weighted sum of two estimates; one conditional on the hypothesis of a maneuver, the other conditional of the hypothesis of no maneuver. The weights are the probabilities that the target is either maneuvering or not, given the latest radar measurement, the sensor noise distribution, uncertainty about the track state estimate, and uncertainty about the target's actual maneuver state. It is not at all clear what constitutes a false alarm or missed detection in a probabilistic predictor.

As long as a deterministic predictor is correct, it produces a better solution than a probabilistic preditor. Conversely, when a deterministic predictor is wrong the probabilistic predictor is better. Probabilistic predictors frequently do better than deterministic predictors. For example, the error statistics show that the IMM consistently outperforms the tracker switching on the position residuals. This is expected because the decisions are based on the same data: the position residuals. However, $c_{\min}$ is such a reliable indicator of a maneuver that it is better to make a determinstic decision than to combine the filter outputs. Although the range rate measurement is hard to interpret and use in a linear filter, it clearly contains enough useful information to improve a track filter.

B. Test Case 2: 1g Maneuver

The ranking of trackers by their error statistics, where the tracker switching on $c_{\min}$ performs best and the tracker switching on the position residuals demonstrate the worst performance, is observed over a wide

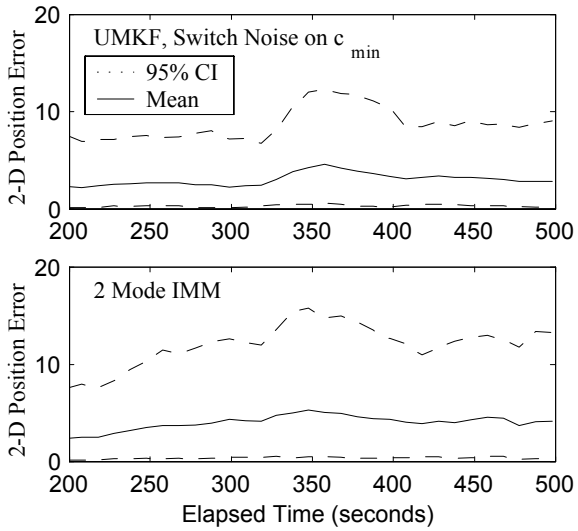

Figure 13: Mean and 95% confidence bounds of position error for the target in test case 2. From top to bottom (i) mode switching tracker using $c_{\min}$; (ii) 2 mode IMM tracker.

range of target characteristics. In this section, the comparison is between the $c_{\min}$ tracker and the IMM only.

In the second scenario, the target starts at time 0 and travels at $350kn$ on a heading of 30°. After $300s$ the target is $75nmi$ from the radar. It makes a coordinated turn to the left with a $1g$ acceleration for $40s$, and then travels straight for 160 s as shown in figure 12. The position and speed errors are shown in in figures 13 and , 14, respectively.

In the first scenario, the acceleration was much larger and the $c_{\min}$ threshold and the maneuver was always detected immediately. In this scenario, the acceleration equals the threshold. It was stated in sections II and III that $c_{\min}$ tends to underestimate acceleration. The $c_{\min}$ tracker is expected be less efficient at detecting this maneuver. In 100 simulation runs, the maneuver is detected on the first scan after it starts only 3 times and by the second scan only 5 times. It is not until third scan that is detected more than 80 times.

As seen in figure 13, the $c_{\min}$ tracker has lower position errors than the IMM. The IMM error variances during the maneuver increase more in this test case than in the other. The maneuver is smaller, so the weight on the maneuver mode increases slowly. Even though the $c_{\min}$ tracker does not reliably detect the maneuver until the third scan after it starts, its errors are lower because it has a better solution at the time the track starts maneuvering. Its error means and variances increase at a faster rate than the IMM's during the first half of the maneuver because the test of $c_{\min}$ fails to detect the maneuver. However, they are consistently lower than the IMM error variances before, during and after the maneuver.

The $c_{\min}$ tracker speed errors are very low before the maneuver because there are so few false alarms, as shown in figure 14. For the next two scans, its speed error stays low because the tracker is in the nonmaneuvering mode. At the third scan, when the maneuver is detected, the tracker switches to the maneuvering mode and the velocity estimate increases to account for the large change in the position estimate. In both trackers, the speed estimate tends to decrease just after the maneuver starts. Eventually, the

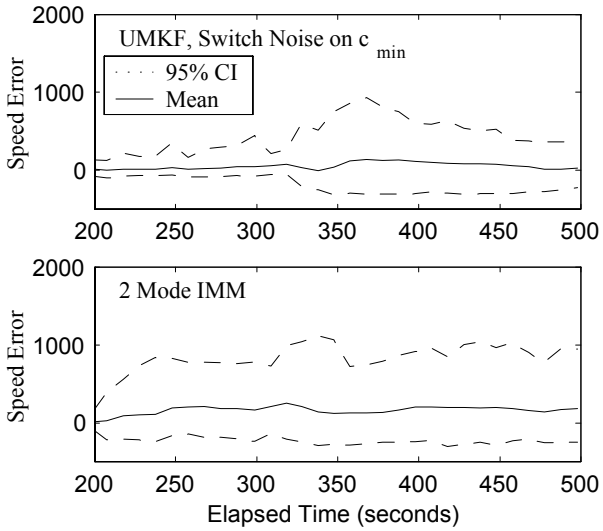

Figure 14: Mean and 95% confidence bounds of speed error for the target in test case 2. From top to bottom (i) mode switching tracker using $c_{\min}$; (ii) 2 mode IMM tracker.

errors become so large that the track speeds back up to catch up to the target.

After the maneuver the target travels near cross-radially with respect to the radar. This is a difficult tracking scenario, and neither tracker's error variances converge back to the values they had before the maneuver started. Their position errors stabilize 50 to 80s after the maneuver ends. The $c_{\min}$ tracker speed error variance tends to decrease because the statistical test usually indicates that the target is not maneuvering. The IMM speed error variance increases slightly because the maneuver mode weight is significant. This example shows the advantage of detecting maneuvers with a statistic that is independent of the position measurements and the current position estimate errors.

5 CONCLUSIONS

The radar range rate measurement can be used to detect maneuvers, but most trackers ignore it when filtering the radar measurements. An algorithm that maps the range rate into a statistic of accelerations under a coordinated turn model is derived. The statistic, called $c_{\min}$, can be interpreted as the minimum acceleration that could have acted on the target to yield the measured range rate, given the previous state estimate. The mapping is nonlinear and nonunique, so the distributional form of the measurement errors are not preserved under transformation. The distribution function of the statistic must be determined via simulation.

This statistic of accelerations turns out to be a reliable indicator of a maneuver. Simulation results, and a direct comparison or receiver operating characteristics, show that a threshold test of $c_{\min}$ is a better predictor of a maneuver than a threshold test against a fading memory average of the position measurement residuals.

Simulation results also show that the $c_{\min}$ tracker outperforms a two mode interacting multiple model tracker. It has lower position and speed error means and variances over a wide range of target characteristics. The range rate measurement contains more information about the target's maneuver state than the position measurement residuals. It contains enough information that a tracker making a deterministic decision about the maneuver state can do better, on average, than one making a probabilistic decision.

6 Acknowledgements

The authors would like to thank Dr. Roman Krzysztofowicz for his help in motivating and formulating the problem.

7 Bibliography

[1] Kameda, H., Tsujimichi, S. and Kosuge, Y., *Target Tracking Using Range Rate Measurement Under Dense Environments*, Electronics and Communications in Japan, Part I, Communications, vol. 85, pp19-29 (2002)

[2] Schutz, R., McAllister, R. and Engleberg., B., *Combined Kalman Filter and JVC Algorithms for AEW Target Tracking Applications*, SPIE Conference on Signal and Data Processing of Small Targets vol. 3163, pp164-175 (July 1997)

[3] McIntyre, G.A. and Hintz, K.J, *Comparison of Several Maneuver Tracking Models*, SPIE Conference on Signal Processing, Sensory Fusion, and Target Recognition VII, vol. 3374, pp48-63 (Apr 1998)

[4] Lee, H., Tahk, M., *Generalized Input-Estimation Technique for Tracking Maneuvering Targets*, IEEE Transactions on Aerospace and Electronic Systems, vol. 35, no. 4, p1388-1402 (Oct 1999)

[5] Mazor, E., Averbuch, A., Bar-Shalom, Y. and Dayan, J., *Interacting Multiple Model Methods in Target Tracking: A Survey*, IEEE Transactions on Aerospace and Electronic Systems, vol. 34, no. 1, pp103-123 (Jan 1998)

[6] Bar-Shalom, Y. and Li, X., *Multitarget-Multisensor Tracking: Principles and Techniques*,

[7] Bizup, D., *A Centripetal Acceleration Statistic for Tracking Maneuvering Targets with Radar*, Proceedings of the 7th International Command and Control Research and Technology Symposium (2002)

[8] Bar-Shalom, Y., *Negative Correlation and Optimal Tracking with Doppler Measurements*, YBS Publishers (1995)

[9] Schutz, R., McAllister, R. and Engleberg., B., *Maneuver Tracking Algorithms for AEW Target Tracking*

Applications, SPIE Conference on Signal and Data Processing of Small Targets vol. 3809, pp308-319 (July 1999).